UDC 616-003.93-085:617-089.844 **doi:** https://doi.org/10.15407/ubj98.04.108

# ACELLULAR DERMAL MATRIX FOR CHRONIC WOUND TREATMENT: DRY OR WET?

*A. I. DOVHALIUK[1], O. I. KULIANDA[2], N. V. OHINSKA[1], O. S. REDKO[1], O. O. KULIANDA[3], A. O. KOVALCHUK[4], V. V. KULBITSKA[1], S. B. KRAMAR[1], Z. M. NEBESNA[1], M. M. KORDA[2], O. O. SHEVCHUK[5]✉*

[1]*Department of Histology and Embryology, Ivan Horbachevsky Ternopil National Medical University, Ternopil, Ukraine;*
[2]*Department of Medical Biochemistry, Ivan Horbachevsky Ternopil National Medical University, Ternopil, Ukraine;*
[3]*Department of Pathophysiology, Ivan Horbachevsky Ternopil National Medical University, Ternopil, Ukraine;*
[4]*Central Research Laboratory, Ivan Horbachevsky Ternopil National Medical University, Ternopil, Ukraine;*
[5]*Department of Pharmacology and Clinical Pharmacology, Ivan Horbachevsky Ternopil National Medical University, Ternopil, Ukraine;*
✉*e-mail: shevchukoo@tdmu.edu.ua*

**Received:** 27 May 2026; **Revised:** 19 June 2026; **Accepted:** 27 July 2026

***Background.*** *Chronic wounds pose a serious clinical and economic burden, and their effective treatment requires the development of new biomaterials that promote tissue regeneration. Acellular dermal matrices (ADMs) represent a promising regenerative strategy; however, their biological properties largely depend on the manufacturing protocol.* ***Objective.*** *To compare the biocompatibility and cytotoxicity of two porcine acellular dermal matrix variants, dry (d-ADM) and wet (w-ADM), and to evaluate the therapeutic efficacy of the biocompatible matrix in an experimental porcine model of chronic full-thickness wounds.* ***Methods.*** *Biocompatibility was assessed in vitro using human umbilical cord-derived mesenchymal stem cells (hU-MSCs) by evaluating cell morphology, viability, proliferation, and lactate dehydrogenase (LDH) release. The therapeutic efficacy of the selected ADM was investigated in a porcine chronic full-thickness excisional wound model and compared with non-adhesive dressings and Promogran Prisma. Wound healing was evaluated after 28 days using histological, immunohistochemical (TNF-α, TGF-β, Ki-67), and morphometric analyses.* ***Results.*** *The wet ADM preserved hU-MSC morphology, viability, and proliferative capacity, whereas the dry ADM induced marked cytotoxicity, increased LDH release, and extensive cell death. In vivo, treatment with w-ADM significantly accelerated wound healing compared with both control dressings, resulting in complete and stable re-epithelialization, minimal inflammatory infiltration, organized collagen remodeling, and improved tissue architecture. Immunohistochemical analysis demonstrated significantly lower expression of TNF-α, TGF-β, and Ki-67, indicating resolution of inflammation and transition toward tissue remodeling and regenerative stabilization.* ***Conclusions.*** *Wet acellular dermal matrix demonstrated excellent biocompatibility and superior regenerative performance, whereas the dry matrix exhibited unacceptable cytotoxicity. Wet ADM represents a promising scaffold for regenerative treatment of chronic wounds and warrants further investigation as a clinically applicable biomaterial, including in combination with mesenchymal stem cell-based therapies.*

*K e y w o r d s: chronic wounds, acellular dermal matrix, lyophilization, human umbilical mesenchymal stem cells, biocompatibility, cytotoxicity, morphology.*

The number of patients with chronic wounds of various origins continues to grow, posing medical and economic challenges to society and the healthcare system [1-3]. Chronic wounds are defined as those with a duration of 3 weeks or longer, or if the wound was referred to as chronic or complex, even with no mention of duration. The definition of “Hard-to-Heal” wounds includes a broader,

more functional/clinical definition used to describe wounds that are not healing as expected, despite standard treatment [4, 5]. As of today, in the global burden for skin and subcutaneous diseases, chronic wounds are not separated, but their prevalence is estimated at 1.67 per 1000 people [CI: 0.83–2.80] and varies from 1.51 to 2.21 per 1000 people depending on the origin [1, 6]. Diabetic ulcers, venous trophic ulcers and pressure sores are the most common causes for chronic wounds [6-8]. According to meta-analysis (2019), chronic wounds prevail in women aged around 70–80 years, in general, among people older than 60 years [9].

Chronic non-healing wounds significantly reduce quality of life and lead to prolonged disability with a substantial financial burden [7, 10, 11]. The health care-related costs of chronic wounds in Australia are approximately 2% of national health care expenditure, more than AUD 3.5 billion [2]. In the USA, total Medicare spending for all wound types reportedly ranges from $28.1 billion to $96.8 billion [8].

In chronic wounds, natural healing processes are impaired due to infections, poor blood supply and reduced tissue regenerative capacity. Conventional treatment methods, including surgery, dressings and pharmacotherapy, often prove insufficient, particularly in cases of extensive or deep injuries [3, 12]. Consequently, modern medicine actively explores novel therapeutic approaches that can stimulate tissue regeneration and accelerate the healing of various types of wounds [1, 13-15].

Today, four stages are recognized in wound healing: hemostasis, inflammation, proliferation and remodeling. Some authors merge hemostasis and inflammation [3, 12, 16]. Stages of proliferation (angiogenesis, growth, re-epithelialization) and remodeling require active involvement of extracellular matrix (ECM), which consists of proteoglycans, hyaluronic acid, collagen and elastin. And today, more than 700 artificial wound dressings are recommended for treating skin defects, and the development of new wound coverings remains robust [14, 17, 18]. Modern biomaterials can actively influence wound healing via absorbing exudate, removing excess fluid, maintaining surface moisture, facilitating gas exchange, maintaining appropriate temperature and/or pH, and preventing additional mechanical trauma to tissues [14, 19].

Acellular dermal matrices (ADMs), essentially a type of extracellular matrix, are increasingly used in healthcare to speed up skin regeneration and for wound treatment [5, 19]. Such biomaterials enhance wound healing compared to the current treatment standards via enhanced vascularization, immunomodulation and microbial protection [20, 21]. ADM is produced by decellularized skin grafts, removing cells and cellular debris while preserving the extracellular matrix structure and protein components as much as possible to support tissue regeneration. These matrices can be derived from donated human or animal skin and are used as “templates” to restore damaged skin and muscle tissues [22, 23]. The main advantage of acellular matrices is their ability to support the natural wound-healing process. They provide mechanical support, reduce inflammation and infection risks, and stimulate angiogenesis. ADM also helps retain wound moisture, creating optimal conditions for tissue regeneration. In chronic wounds, where natural healing is disrupted, using acellular matrices can be crucial in successful tissue restoration [24, 25].

Hsieh et al. reported that hydrogel-treated wounds were closed by day 14, without inflammation. Additionally, dermal fibroblast infiltration and regeneration of hair follicles and sweat glands were observed, as opposed to the control group [26]. Tognetti et al. achieved complete healing of a deep post-traumatic wound of the foot in 7 weeks using human ADM [27]. Brown et al. demonstrated that ADM-based hydrogels improved diabetic wound healing [28].

Hard-to-heal wounds have become particularly relevant in Ukraine since the full-scale russian invasion [29-31]. We are dealing not only with quite common chronic wounds at diabetic feet, venous ulcers and pressure sores, but with wounds with tissue deficiency, lack of muscles and bones due to blast injuries and traumatic amputations. Long evacuation from the battlefield leads to bacterial contamination, including multidrug-resistant flora, and negatively affects the healing process. These devastating wounds present a therapeutic challenge to restore the protective skin barrier and preserve tendon and muscle excursion, provide protective padding around nerves and restore adequate joint motion [32].

The aim of our study is to compare the cytotoxicity and biocompatibility of two variants of porcine acellular dermal matrices: dry ADM (d-ADM) and wet ADM (w-ADM), and to evaluate the real therapeutic efficacy of the best ADM in an experimental model of chronic wounds, both clinically and morphologically.

## Materials and Methods

*Ethics statement.* All experimental procedures involving animals were conducted in accordance with internationally recognized bioethical standards and principles of the European Convention for the Protection of Vertebrate Animals used for Experimental and other Scientific Purposes (Strasbourg, 1986) and the study was approved by the Bioethics Committee (protocol No. 80 dated January 10, 2025) of the Ivan Horbachevsky Ternopil National Medical University.

*Preparation of porcine decellularized dermis matrices variants.* Porcine skin was used to create acellular xenografts. The skin was harvested industrially. Animals were sourced from a commercial farm operating under routine veterinary supervision. Prior to inclusion in the study, all pigs underwent veterinary examination and were certified as clinically healthy, with no evidence of infectious or parasitic diseases. Only animals meeting these health criteria and accompanied by official veterinary documentation were enrolled in the study. Within two hours of harvesting, the epidermal layer (0.3–0.4 mm of thickness) was removed using a dermatome, followed by a second layer (1–1.2 mm thick), which underwent physical and chemical processing. Decellularization of dermis samples was performed in four main steps [18]:

1. Freeze-thaw cycles: Samples were alternately submerged in liquid nitrogen (–196) °C and warm water +37°C three times.

2. Glycerin dehydration: Samples were soaked in glycerin for 3 h.

3. Osmotic stress: Alternating immersion in distilled water and hypertonic solution.

4. Detergent treatment: Samples were processed with a 1 M NaOH solution for 1 h, followed by removal of cellular debris using 1% SDS.

The effectiveness of the decellularization protocol was assessed histologically at each step, as previously published [18, 33]. Post-detergent treatment, dermis pieces underwent either freeze-drying in a lyophilized (dried version of ADM, d-ADM) or immersion in a triple solution (500 g $CaCl_2$ + 648 ml of distilled water + 518 ml of ethanol) heated to 75°C for 1 h using a water bath (wet version of ADM, w-ADM). Sterilization of the resulting decellularized matrices was performed using ultraviolet radiation. Matrices were stored at room temperature in craft envelopes (d-ADM) or as a 1:1 mixture of glycerin and phosphate buffer at 4°C (w-ADM) (Fig. 1).

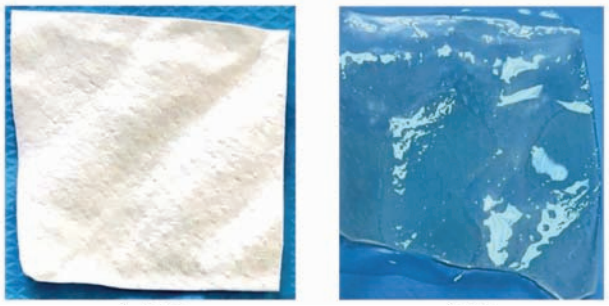


*Fig. 1. Dry (d-ADM) and wet (w-ADM) of acellular dermal matrix*

*Isolation and cultivation of hU-MSCs.* A hU-MSC line was used for biocompatibility and cytotoxicity assessment. Primary hU-MSC cultures were isolated enzymatically from umbilical cord tissue (following physiological childbirth with informed patient consent) using collagenase I (Gibco, Thermo Fisher Scientific, US) at a 0.075 mg/ml concentration. Dissociated cells were cultured in Advanced DMEM/F12 medium (Gibco, Thermo Fisher Scientific, US) with 10% fetal bovine serum (FBS) (Gibco, Thermo Fisher Scientific, US) at passage 0. In subsequent passages, FBS concentration was reduced to 2%. Cultures were maintained at 37°C in a $CO_2$ incubator with 5% $CO_2$.

Immunophenotyping was conducted at passage four via flow cytometry (Invitrogen monoclonal antibodies, Thermo Fisher Scientific, US) and revealed approximately 98% CD73+, CD90+, CD105+, CD34–, and CD45– cells. According to the International Society for Cellular Therapy (ISCT) 34, it confirmed mesenchymal lineage. Cytogenetic analysis in passage 5 showed no statistically significant increase in spontaneous mutations compared to primary culture.

*Experimental design for assessing biocompatibility and cytotoxicity of ADMs.* Passage-4 cells were used for experiments. The study was conducted in triplicate. To evaluate the biocompatibility and cytotoxicity of d-ADM and w-ADM, 6-well culture plates (Nunclon Delta Surface, Thermo Fisher Scientific, USA) were used. Each well was seeded with 100,000 cells in 2 ml of growth medium (DMEM/F12 Advanced + 2% FBS). Simultaneously, 1 $cm^2$ dermal matrix pieces (pre-washed in distilled water and phosphate buffer) were added to 3 wells per plate, while the remaining three wells served as negative controls (without matrices). The cultures

were maintained for 5 days in a $CO_2$ incubator, with daily assessments of hU-MSC morphology and population density (confluence) using an inverted microscope (Delta Optical, Poland).

Biocompatibility was assessed based on cell condition and proliferation rates, with cell growth analyzed after 5 days. Direct cytotoxicity was determined by calculating the viability index, which is defined as the ratio of live cells to total cells harvested from each well at the end of the experiment. Cell counts were performed using a hemocytometer and 0.4% trypan blue vital stain. Indirect cytotoxicity was assessed via lactate dehydrogenase (LDH) activity in the conditioned medium supernatant [34].

The conditioned medium for determining LDH activity was collected from the wells of the culture plates on the 5$^{th}$ day of the experiment, before counting the cells. The supernatant of the conditioned medium was stored at 4°C in tightly sealed tubes for 2–3 days until LDH concentration measurement. For the positive cytotoxicity control, 100,000 cells were seeded into each well of a separate plate, and 20 µl of the lytic agent Triton X-100 was added to each well one hour before the end of the experiment.

*LDH cytotoxicity assay.* LDH activity in supernatants was measured spectrophotometrically at 340 nm using 10-mm path-length cuvettes. The kinetic UV method was performed on a Lambda 25 spectrophotometer (Perkin Elmer, USA) per the instructions of the LDH detection kit (Felicit Diagnostics, Ukraine). The method is based on the LDH-catalysed reaction:

$$\text{Pyruvate} + \text{NADH} + H^+ + \text{LDH} \rightarrow$$
$$\rightarrow \text{Lactate} + NAD^+.$$

The decrease in absorbance at 340 nm, associated with NADH oxidation, is directly proportional to LDH activity in the sample [35]. Negative controls used supernatant of the conditioned medium from wells without ADM. As a positive cytotoxicity control, the supernatant from wells treated with Triton X-100 was used to measure the maximum LDH release, which occurs upon the destruction of all cells. Optical density measurements of the samples were conducted at a temperature of 25°C.

*Cytotoxicity index calculation.* The cytotoxicity index (CTI) was calculated using the formula:

$$CTI = (A_{exp}\ LDH/A_{max}\ LDH) \times 100\%,$$

where $A_{exp}$ LDH is the experimental LDH activity (U/l), and $A_{max}$ LDH is the maximum LDH activity of positive controls (U/l).

*Statistical analysis.* LDH activity tests for each control and matrix variant were performed in eight replicates. The mean change in light absorbance (ΔA/min) values for test solutions was converted into LDH activity (U/l) using the formula: ΔA/min×4925 = U/L LDH. Mean square values and 95% confidence intervals were calculated. Differences were considered significant at $P < 0.05$.

*Modelling of a full-layer wound.* White pigs with a body mass of 15 kg were used for experimental studies. The animals were kept in vivarium conditions following international care principles and experimental research using laboratory animals.

The experiment (modelling impaired excisional wound) was performed under thiopental sodium anaesthesia (80 mg/kg, intramuscularly). Full-thickness wounds were created on the back of pigs by excising the skin and subcutaneous adipose tissue down to the level of the superficial fascia using a scalpel. Wounds of a size of 5 × 5 cm were on both sides of the spine. Bilateral wounds were formed on both sides of the spine, with a minimum distance of 4 cm between them [36]. To limit spontaneous wound contraction and ensure a consistent wound area over time, incisions were made to disrupt actomyosin fibres, thereby reducing the contractile activity of the wound edges [37, 38]. Without such intervention, full-thickness wounds in this model tend to contract and close spontaneously by day 28, regardless of the local treatment method (Fig. 2).

Wound No.1 was covered with the non-adhesive aseptic dressing.

Wound No.2 after the formation was covered with Promogran Prisma (3M™ Promogran Prisma™ Matrix; Systagenix, Gargrave, UK), a collagen wound matrix consisting of a sterile, freeze-dried

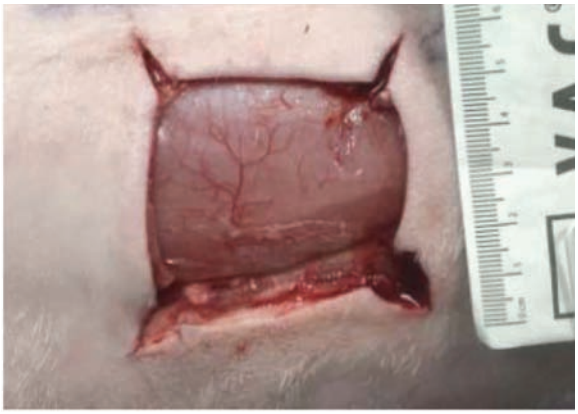

*Fig. 2. The modeled uncovered wound on a pig*

balanced combination of 44% oxidized regenerated cellulose, 55% collagen and 1% silver.

Wound No.3 was covered with a porcine wet acellular dermal matrix (w-ADM).

All wounds were additionally covered with adhesive dressings for better fixation.

The morphological assessment of wound healing and biopsy from central and marginal areas of the wounds was performed in 28 days.

*Morphological studies.* Tissue samples were fixed in a 10% neutral buffered formalin solution. Further processing was carried out using a LOGOS ONE tissue processor, and paraffin blocks were made using a TEC 2800 tissue embedding station. Thin sections of 5-6 μm thickness obtained on a manual rotary microtome AMR 400 were stained with hematoxylin and eosin, azan III with chromium. The histological specimens were examined using a MICROmed SEO SCAN light microscope and photo-documented using a Vision CCD Camera with an image output system for histological specimens.

*Immunohistochemical studies.* Immunohistochemical studies were performed on paraffin sections (4 μm thick) of skin from the central and marginal wound areas. The process of deparaffinization and recovery of antigens was carried out in Target Retrieval Solution buffers (Agilent Technologies, USA) with low (6) or high (9) pH in a KOS multifunctional microwave tissue processor (Milestone, Italy).

The following rabbit polyclonal primary antibodies were used for immunohistochemical detection of target proteins:

- Anti-TGF beta-1 (PA5-145251, Invitrogen, USA);
- Anti-TNF alpha (BS-0078R, Invitrogen, USA);
- Anti-Ki-67 (ab16667, Proteintech, USA) for Ki-67+ cells.

Secondary antibodies were part of the Mouse/Rabbit PolyVue™ HRP/DAB detection system (Diagostic BioSystems, USA). Counterstaining of the sections was performed with Mayer's hematoxylin (Biognost, Croatia).

*Morphometric studies.* Quantitative assessment of the results of immunohistochemical studies was performed in ImageJ software by processing the documented histograms using the functions "Color Deconvolution", "Threshold" and "Analyze Measure". Morphometrically, the epidermis' thickness and the number of fibroblastic cells per unit area were also determined in the wound's marginal and central regions. For the data obtained within one group, the arithmetic mean (M), the error of the arithmetic mean (m), and the standard deviation were determined (σ). The normal distribution determined the reliability of the difference between the data according to Student's *t*-test. Differences were considered significant at a value of $P < 0.05$.

## Results

*Evaluation of the biocompatibility and potential cytotoxicity of the two variants of acellular dermal matrices (ADMs)*

Our first step was to identify the cytotoxicity and biocompatibility of two variants of porcine ADMs, dry (d-ADM) and wet (w-ADM). *In vitro* co-cultivation of human umbilical-derived mesenchymal stem cells (hU-MSCs) with the corresponding xenogeneic biomaterial was used.

We analyzed the morphological changes, proliferation rates, viability of cultured cells, and levels of Lactate Dehydrogenase (LDH) released by damaged cells into the conditioned medium. In the presence of w-ADM, hU-MSCs maintained their shape and proliferative activity, compared to the control group (Fig. 3, *A*, *B*; Table 1). In contrast, d-ADM had a pronounced inhibitory effect on the viability of cultured cells. Only a few MSCs were observed along the edges of the wells in this variant (Fig. 3, *C*), while dead cells were detected near the acellular dermis (Fig. 3, *D*).

The MSC viability index on day 5 did not differ between the control and w-ADM groups (Fig. 4, *A*). The negative impact of dry dermis on cultured MSCs was evident in a 12.8-fold reduction in the number of live cells in wells containing d-ADM (Fig. 4, *B*).

The viability index of hU-MSCs is a critical marker of the biocompatibility of xenogeneic dermal matrices with human cells. This indicator is a direct test of the material's cytotoxicity. However, some researchers recommend conducting an additional indirect cytotoxicity test based on the levels of LDH in the medium [39]. LDH is rapidly released into the cell culture supernatant when the plasma membrane is damaged. This index is a biomarker of cell damage, including apoptosis and necrosis [39]. The total LDH activity in wells with d-ADM was over 9 times higher than the control level (Fig. 4, *B*). This sharp increase positively correlates with the number of dead cells and indirectly witnesses the toxic effect of

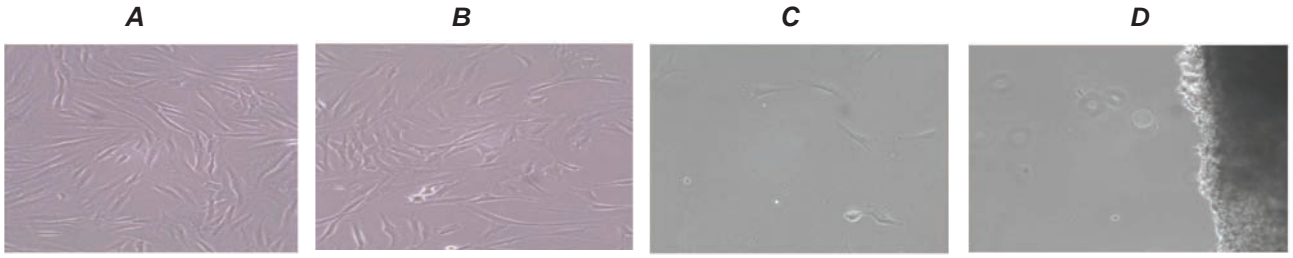


*Fig. 3. Morphology and population density of hU-MSCs cultured in the presence of decellularized dermal samples on day 5 of the experiment. 100× magnification.* ***A*** *– Control;* ***B*** *– MSCs in a well with w-ADM;* ***C*** *– MSCs along the edge of a well with d-ADM;* ***D*** *– Dead cells near d-ADM*

*Table 1. Cell population density in culture wells with and without the presence of ADM at different experimental time points*

| Timepoint | Control | d-ADM | w-ADM |
|---|---|---|---|
| Day 1 | 15% | 5% | 12% |
| Day 3 | 40% | 0–1% | 38% |
| Day 5 | 65% | 0–1% | 60% |

the d-ADM matrix. In contrast, this indicator for the wells with w-ADM did not statistically differ from the control group.

The next step of the study was to estimate the effectiveness and efficiency of the w-ADM experimentally on the modelled full-layer wound. On the 28th day, we compared the wound healing process of wounds covered by non-adhesive aseptic wound dressing, Promogran Prisma matrix and w-ADM.

*Structural changes of the full-layer wound covered with a non-adhesive aseptic wound dressing.* Histology showed that a covering with a non-adhesive aseptic dressing did not promote the epithelization of the full-layer wound in 28 days. We observed granulation tissue with intense mononuclear infiltration and extensive interstitial haemorrhage; vessels with sludge effect and erythrocyte stasis. It corresponded to the second phase of granulation formation (Fig. 5.1, *A*). In the deeper layers of the dermis, a phase of partial remodeling occurred (fibre components were destroyed, often fragmented, homogenized); areas of their disintegration (Fig. 5.1, *B*). Fibroblastic cells were elongated with eosinophilic cytoplasm, their nuclei were intensely basophilic, often with signs of pyknosis (Fig. 5.1, *C*). Morphometry found that the number of fibroblast cells was (538 ± 25) cells/mm$^2$. Histoleukocyte infiltrates formed clusters, or they were diffusely lo-

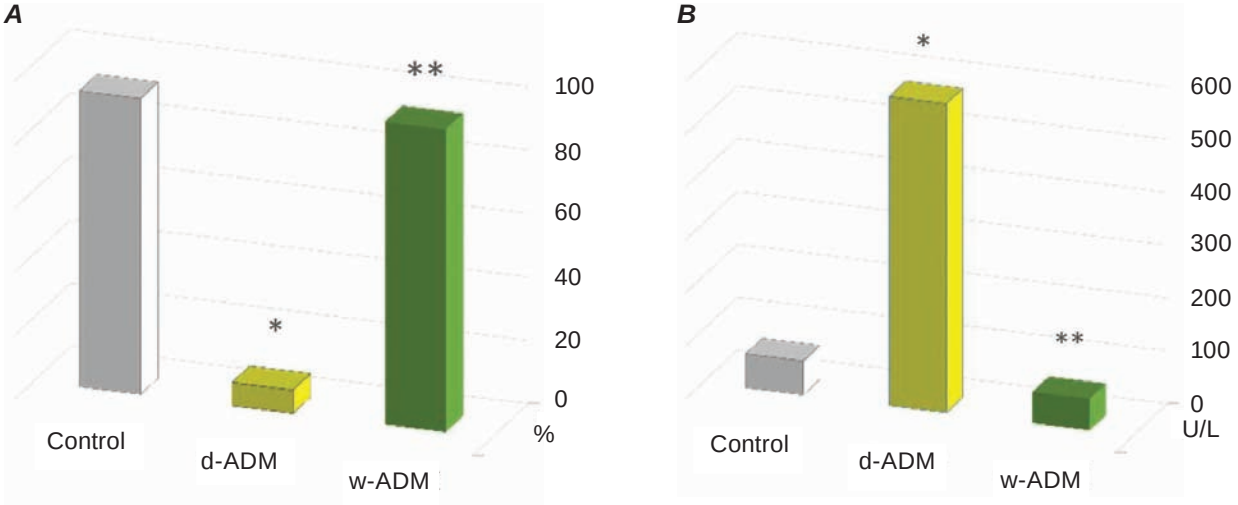


*Fig. 4.* ***A*** *– Viability index of hU-MSCs with and without the presence of ADM, showing % of living cells.* ***B*** *– Total LDH activity in the conditioned medium, U/l. *Significant difference compared to control, P < 0.001; **significant difference compared to d-ADM, P < 0.001*

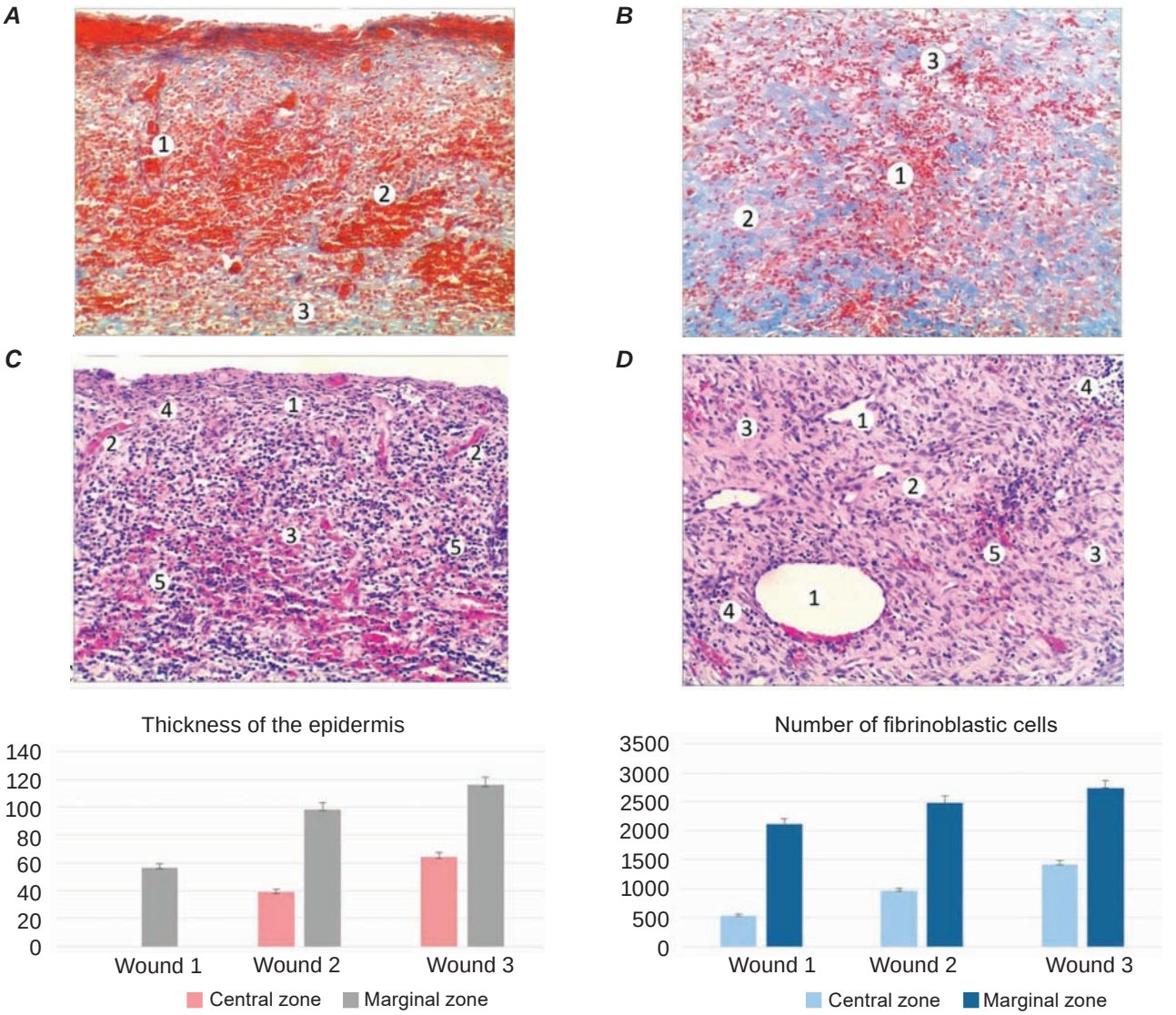


*Fig. 5.1. Microscopic changes in the central area and deep layers of the dermis of full-layer wound No 1 (non-adhesive aseptic wound dressing) after 28 days of experiment. Magnification: x 100.* ***A****: 1 – blood-filled vessels, 2 – hemorrhages, 3 – fibrillar collagen structures. Azan III chrome stain.* ***B****: 1 – diffuse hemorrhages, 2 – collagen fibers in the granulation composition, 3 – newly formed vessels. Azan III chrome stain.* ***C****: 1 – granulation tissue, 2 – full blood vessels, 3 – interstitial hemorrhages, 4 – fibroblasts, 5 – leukocyte infiltration. Hematoxylin and eosin staining.* ***D****: 1 – blood vessels, 2 – granulation, 3 – fibroblasts, 4 – mononuclear infiltration, 5 – hemorrhages. Hematoxylin and eosin staining*

calized between the fibers. In the deeper layers of the dermis, the intercellular substance was oedema with the formation of characteristic slightly oxyphilic light voids (Fig. 5.1, *D*).

In the marginal area of the wound, a thin layer of the epidermis with destructive changes was preserved. Acanthosis with parakeratosis was detected. The epithelial cells of all layers were edematous; as a result, the cells had a clear, slightly oxyphilic cytoplasm, and their nuclei were hyperchromic (Fig. 5.2, *A*). There was a decrease in the layers of epithelial cells in the stratum spinosum layer, their intercellular junctions were disturbed, and pericellular oedema was detected. The epithelial cells of the stratum basale had an irregular shape, their nuclei were pleomorphic, intensely basophilic, and there were no mitotic division figures (Fig. 5.2, *B, C*). The thickness of the epidermis was (56.88 ± 2.81) μm. The inflammatory reaction manifested by the diffuse mononuclear infiltration in the dermis of the peripheral areas

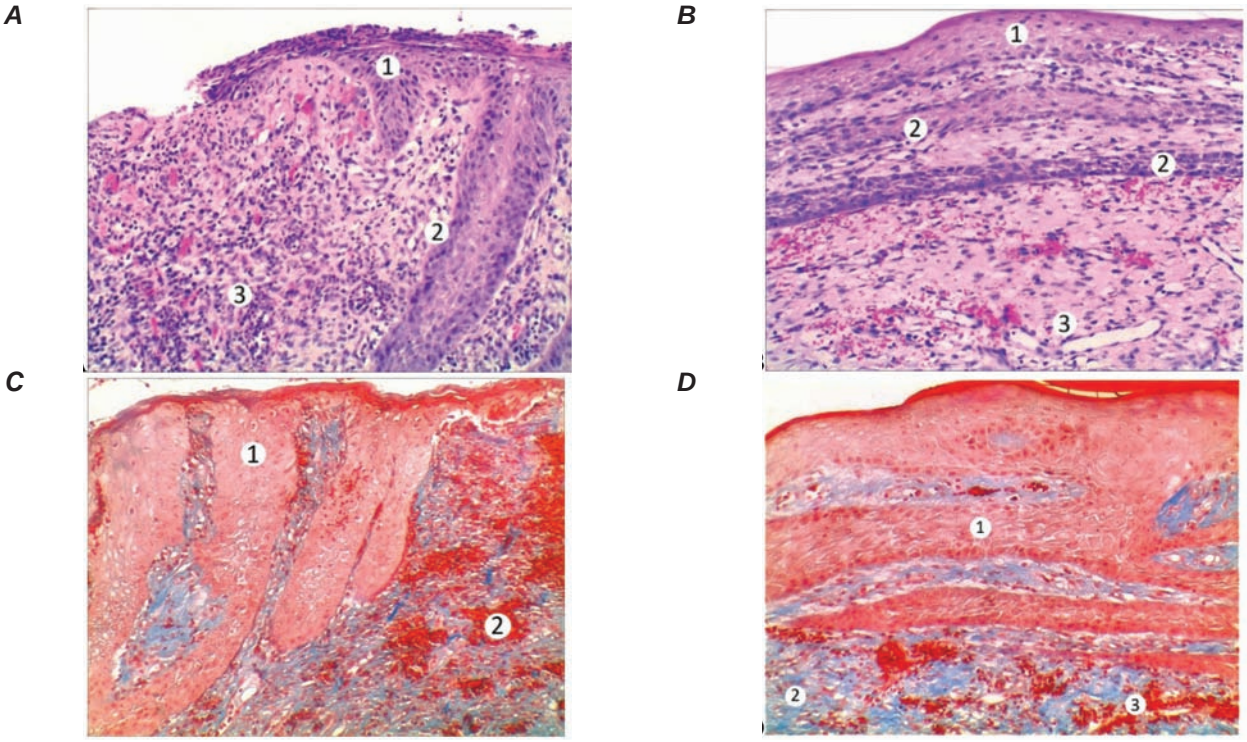


*Fig. 5.2. Microscopic changes in the marginal area of full-layer wound No. 1 (non-adhesive aseptic wound dressing) after 28 days of experiment. Hematoxylin and eosin staining. Magnification: x100.* ***A****: 1 – epidermis, 2 – acanthosis in the form of budding, 3 – infiltrated dermis. Hematoxylin and eosin staining. Magnification: x100.* ***B****: 1 – epidermis, 2 - epidermal invaginations, 3 – vessels in granulations. Hematoxylin and eosin staining. Magnification: x100.* ***C****: 1 – epidermis, 2 – hemorrhages. Azan III chrome stain. Magnification: x100.* ***D****: 1 – epithelial acanthosis, 2 – collagen fibers, 3 – interstitial hemorrhages. Azan III chrome stain*

of skin damage (Fig. 5.2, *A*, *D*). The number of fibroblastic cells in this area was (2115 ± 104) cells/mm$^2$.

*Structural changes of the full-layer wound covered with Promogran Prisma matrix.* Application of Promogran Prisma in 28 days finalized in epithelial regeneration in the central area of the wound, which was uneven and had an unclear stratification. The cells were tightly interconnected, indicating the integrity of the components of intercellular interaction (Fig. 6.1, *A*). The thickness of the epidermis was (39.23 ± 1.92) μm. The intensity and distribution of histoleukocyte infiltration were moderate. Intensely oxyphilic interstitial hemorrhages were diffusely localized (Fig. 6.1, *B*). In the superficial layer of the dermis, there were many hematogenous and fibroblastic cells. The number of fibroblastic cells in this zone was (963 ± 47) cells/mm$^2$. Collagen fibres were in a transformation, forming a network; they were partially fragmented (Fig. 6.1, *C, D*). There was a gradual regression of angiogenesis, and blood vessels were without signs of blood filling, with clearly contoured walls.

In the marginal area, there was reactive epithelial proliferation with subsequent overgrowth and capture of dermal fragments. Often, intracellular edema with characteristic cytoplasmic lucencies was noted in epithelial cells of all layers of the stratified squamous keratinized epithelium, their nuclei were normochromic or hyperchromic (Fig. 6.2, *A*). The thickness of the epidermis was (98.41 ± 4.75) μm. The superficial layer of the dermis contained formed granulation tissue with a low density of fibroblastic cells and a predominance of fibrocytes. Inflammatory leukocyte infiltration was detected diffusely. The fibrous components of the dermis were often swollen, of different thickness and direction, but without signs of disorganisation and fragmentation (Fig. 6.2, *B).* There were a few histiogenic and hematogenic cells, which were located between the fibre structures (Fig. 6.2, *C, D*). The number of fibroblastic cells in this area was (2481 ± 123) cells/mm$^2$.

*Structural changes of the full-layer wound covered with w-ADM.* The application of wet acellular dermal matrix to a full-layer skin defect after 28

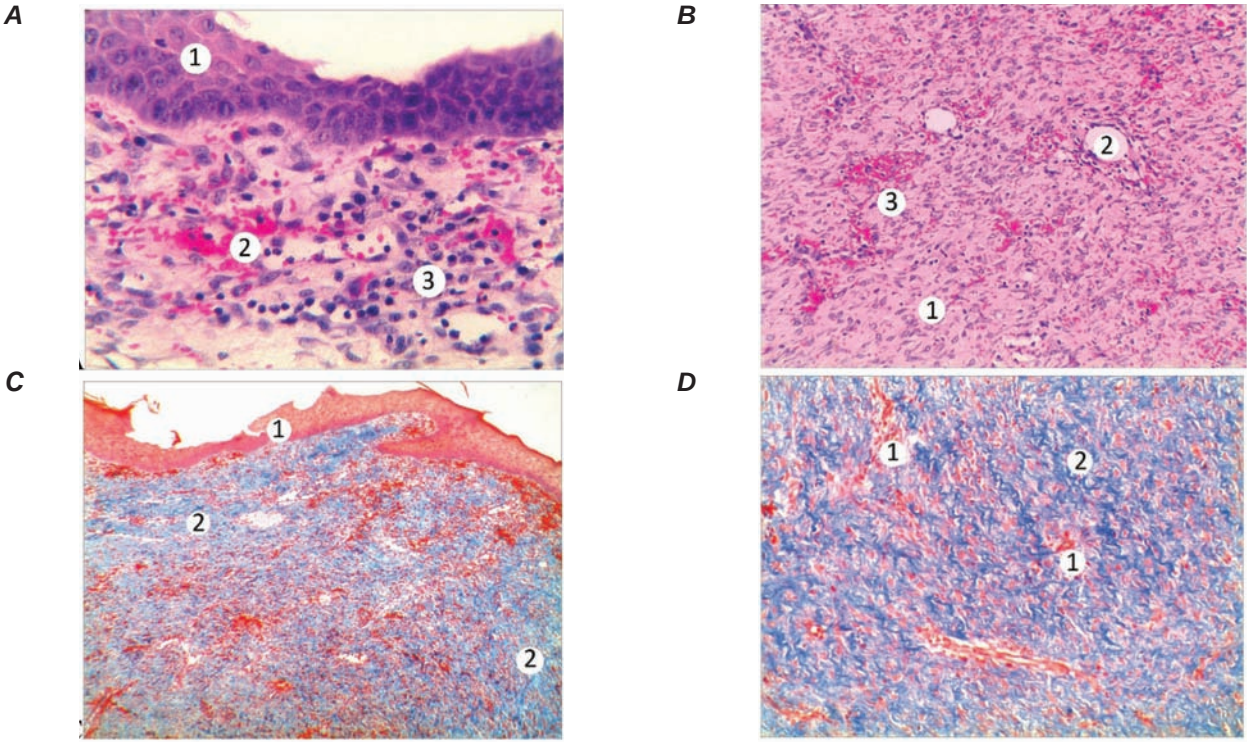


*Fig. 6.1. Microscopic changes in the central area of full-layer wound No. 2 using Promogran Prisma matrix after 28 days of experiment.* ***A****: 1 – epithelium, 2 – hemorrhages, 3 – histoleukocyte infiltration in granulation tissue. Hematoxylin and eosin staining. Hematoxylin and eosin staining. Magnification: x250.* ***B****: 1 – granulation, 2 – blood vessels, 3 – foci of interstitial hemorrhages. Hematoxylin and eosin staining. Hematoxylin and eosin staining. Magnification: x100.* ***C****: 1 – damaged epithelium, 2 – collagen fibers. Azan III chrome stain. Magnification: x100.* ***D****: 1 – hemorrhages, 2 – fibrous structures in the dermis. Azan III chrome stain. Magnification: x100*

days was characterized by a minimal inflammatory reaction in the central area of the wound, complete closure of the wound with epithelial regeneration in the phase of stabilization. The thickness of the epidermis was (64.55 ± 3.12) microns. We observed a restoration of stratification of the stratified squamous keratinized epithelium. The basement membrane was completely restored, keratinocytes were layered and tightly connected by desmosomal intercellular junctions (Fig. 7.1, *A*). In the granulation tissue, erythrocyte diapedeses were single, histoleukocyte infiltration was insignificant, and in most cases, dissociated and scattered. The number of fibroblastic cells in this zone was (1422 ± 70) cells/mm$^2$. Fibroblastic cells were characterized by a typical elongated shape with basophilic nuclei and oxyphilic cytoplasm (Fig. 7.1, *B, C, D*).

The epidermis in the marginal area of the wound had a slightly thickened stratum spinosum layer. The epithelial cells of the stratum basale layer were tightly connected to the basement membrane, had intensely basophilic nuclei and a slightly altered cell shape (Fig. 7.2, *A*). The thickness of the epidermis was (115.97±5.65) microns. In the superficial layer of the dermis, there were local inflammatory accumulations of leukocytes, macrophages, and fibroblasts. There was also a moderate blood filling of the vessels, and erythrocyte diapedesis was single (Fig. 7.2, *B*). Collagen fibres of the connective tissue of the superficial and deep dermis were well expressed, formed multidirectional bundles, and were well visualised by azan III chrome staining. Morphometrically, it was found that the number of fibroblast cells in this zone was (2740 ± 131) cells/mm$^2$ (Fig. 7.2, *D, C*).

*Immunohistochemical study of full-layer wound with different dressings.* Immunohistochemical studies of full-layer wound No. 1 (non-adhesive aseptic wound dressing cover) on day 28 of the experiment with the application of anti-TGF

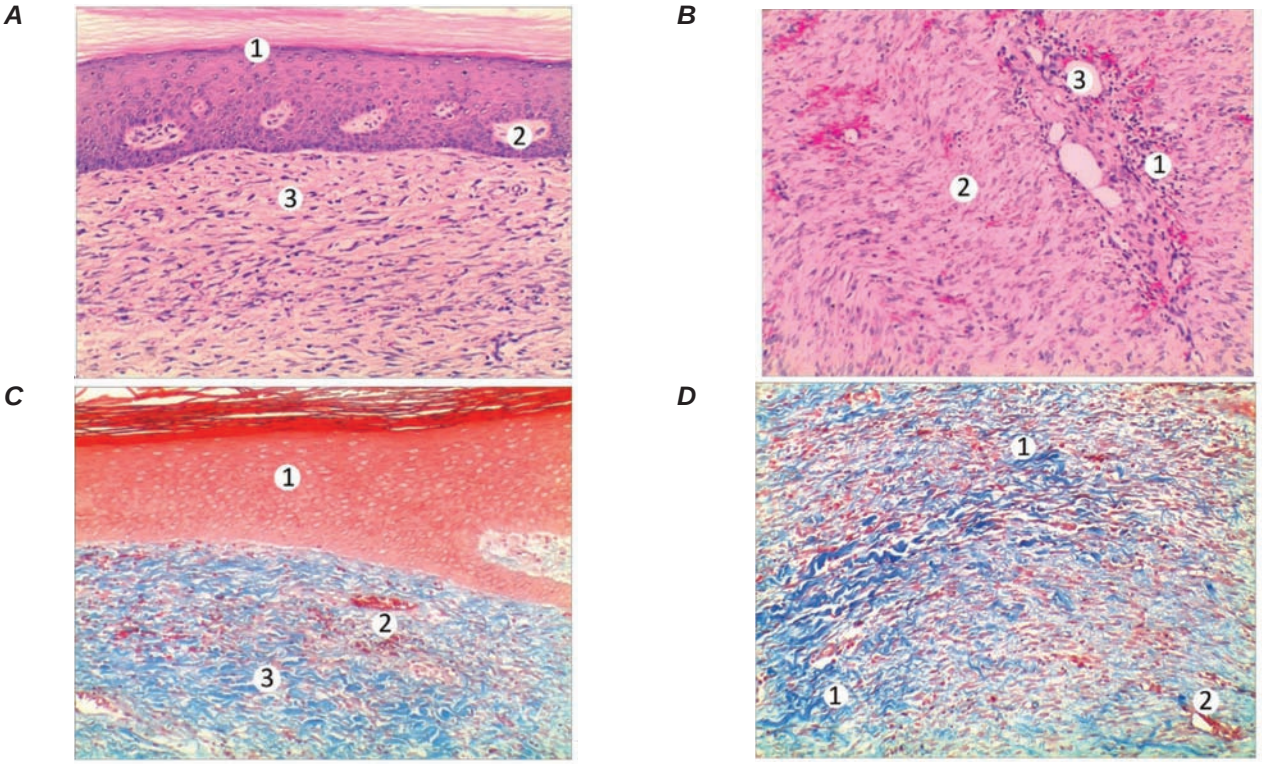


*Fig. 6.2. Microscopic changes in the marginal area of full-layer wound No. 2 using Promogran Prisma matrix after 28 days of experiment. Magnification: x100.* ***A****: 1 – epidermis, 2 – fragments of connective tissue in the epidermis, 3 – mature granulation tissue. Hematoxylin and eosin staining.* ***B****: 1 – histoleukocyte infiltration, 2 – granulation, 3 – blood vessels.* ***C****: 1 – epidermis, 2 – small interstitial hemorrhages, 3 – collagen fibrils. Azan III chrome stain. Magnification: x100.* ***D****: 1 – fibrous structures in the dermis, 2 – blood vessels. Azan III chrome stain*

beta-1 antibodies revealed TGF beta expression at the level of (31.14 ± 3.19)% in the central area, and (23.11 ± 1.44)% in the marginal zone (Fig. 8).

With the use of Promogran Prisma matrix, the expression of TGF beta in the centre of the healing area was (26.34 ± 2.53)%, and in its marginal zone – (20.16 ± 1.03)%, which in both cases did not significantly differ from the indicator of wound No. 1.

When wet acellular porcine dermal matrix was applied to wound No. 3, the percentage of immunohistochemical expression of TGF beta in the center was 18.48 ± 1.67 ($P < 0.01$), while in the marginal areas – 9.07 ± 0.97 ($P < 0.001$), which was significantly lower than the level of expression of this protein compared to wound No. 1 (Fig. 8).

Expression level of the proinflammatory cytokine TNF alpha in the central and marginal areas of wound No. 1 was (43.61 ± 3.57)% and (28.19 ± 1.88)%, respectively. Regarding the wound No. 2 (with Promogran Prisma), this index was in the centre of the injury (29.15 ± 2.83)% ($P < 0.05$), on the periphery (18.18 ± 1.22)% ($P < 0.001$), which was lower than in the wound No. 1 covered with aseptic dressing. Immunohistochemical studies of the main and marginal areas of wound No. 3 covered with w-ADM established the percentage of TNF alpha expression at 22.17 ± 1.84 ($P < 0.001$) and 10.67 ± 1.13 ($P < 0.001$), respectively, which was significantly lower than that of wound No. 1 (Fig. 9).

Anti-Ki-67 antibodies were used to estimate the proliferative activity of cells in the epidermis and dermis of the wounds. The lowest expression of the Ki-67 marker in the Malpighian layer of the epidermis was detected in wound No.1 (11.43 ± 1.92)%, which is associated with the unformed epithelial layer in this group. In full-layer wounds No. 2 and No.3, it was significantly higher ($P < 0.001$). The proliferative activity of epidermal cells in the marginal areas of the injury was: wound No. 1 – (55.74 ± 4.06)%, wound No. 2 – (35.27±3.18)% ($P < 0.01$), wound No. 3 – (28.17±1.81)% ($P < 0.001$) (Fig. 10).

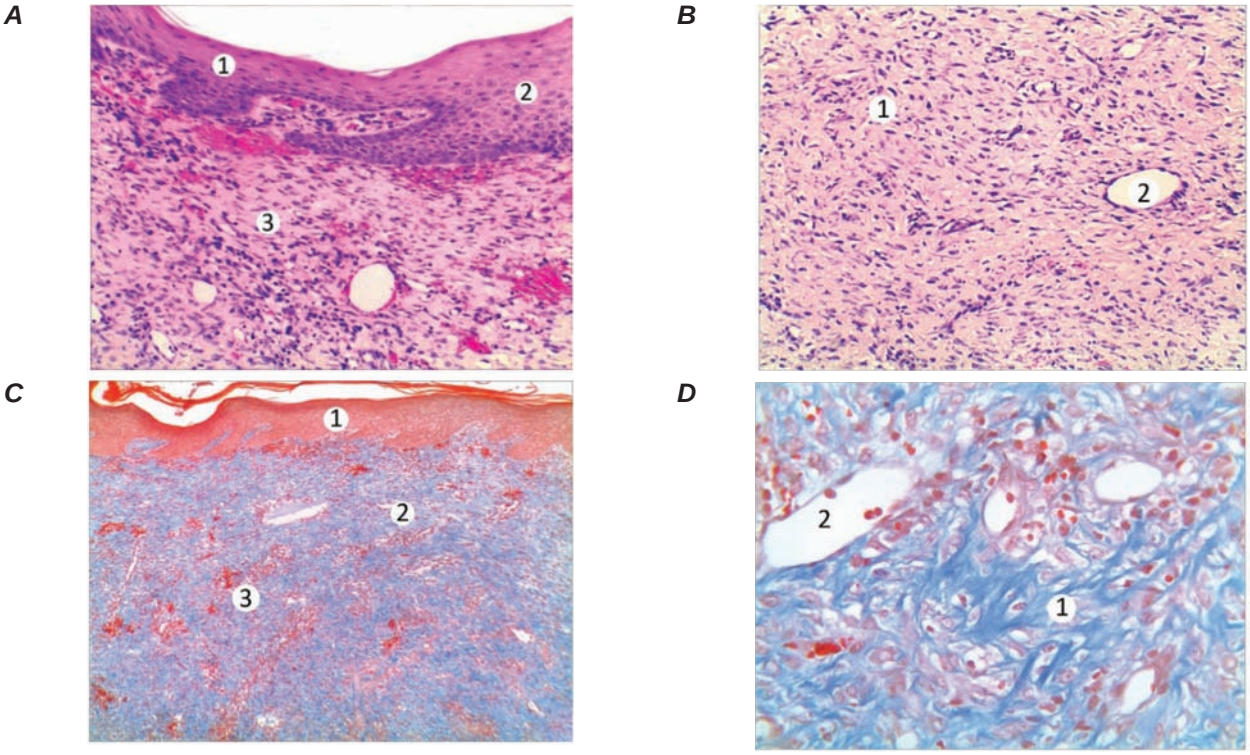


*Fig. 7.1. Microscopic changes in the central area of the full-layer skin defect No. 3 under the conditions of acellular dermal matrix application after 28 days of experiment. Magnification: x100.* ***A:*** *1 – epidermis, 2 – pleomorphic nuclei of the stratum spinosum layer epithelial cells, 3 – granulation tissue. Hematoxylin and eosin staining.* ***B:*** *1 – fibroblasts, 2 – hemocapillaries. Hematoxylin and eosin staining.* ***C:*** *1 – epidermis, 2– blood vessels, 3 – interstitial hemorrhages. Azan III chrome staining. Magnification: x100.* ***D:*** *1 – blood vessels, 2 – collagen fibers bundles. Azan III chrome stain. Magnification: x250*

The mitotic activity of dermal cells in wound No. 1 was (52.79 ± 4.51)% in the central zone and (22.11 ± 1.42)% in its periphery. The expression of Ki-67 in the dermis of wound No. 2 in the central zone was significantly decreased ($P < 0.05$) compared with wound No. 1 (it could serve as a control group) and did not differ in the marginal zone. w-ADM covering showed a significant decrease in the proliferative activity of dermal cells in both the central and marginal areas of wound No 3, (19.97 ± 2.59)% ($P < 0.001$) and (10.87 ± 1.94)% ($P < 0.01$), respectively.

## Discussion

The dermal ECM consists mainly of collagen and elastic fibres (80–85% of the dry weight of dermis), glycosaminoglycans, and proteoglycans. Human skin contains 80–90% of Type I collagen, 8–12% of Type III collagen, and less than 5% of Type V collagen. Type IV collagen is found in the dermal-epidermal junction and surrounds blood vessels, nerves, and skin derivatives. Elastic fibres make up to 2–4% of the dermal ECM and consist of elastin and elastin-associated microfibrils. The gel-like amorphous substance in the dermis includes glycoproteins (fibronectin, fibulin, and integrins), glycosaminoglycans, and proteoglycans, which make up only 0.2% of the dermal dry weight but have powerful hygroscopic properties. Consequently, water constitutes approximately 60% of the total dermal mass [40]. The purpose of decellularization is to remove the immunogenic cellular components while maintaining the intact 3D structure of the matrix. Acellular matrices contain various cytokines and signaling molecules, such as vascular endothelial growth factor (VEGF), fibroblast growth factor (FGF), and TGF-beta [41].

The protocol for creating ADM involves breaking down cellular membranes and nucleic acids and extracting them using various detergents [18]. However, the extracting agents can degrade or denature matrix proteins and cause toxic effects.

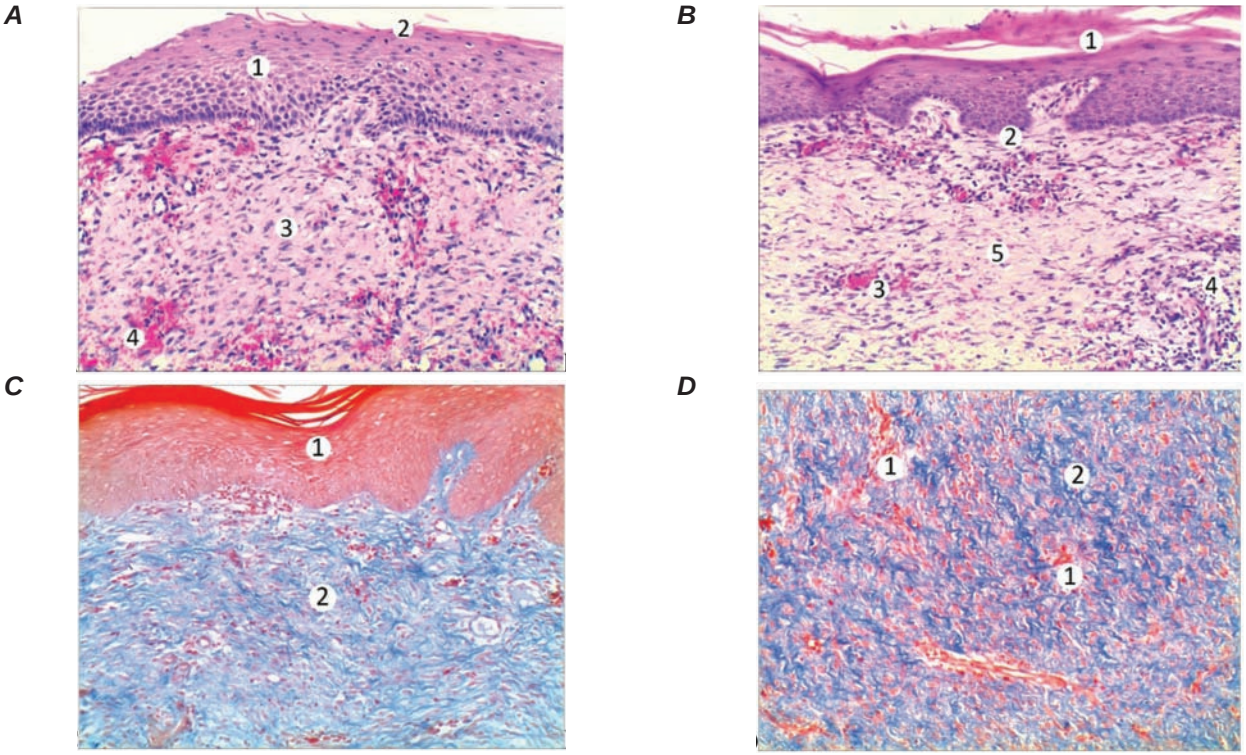


*Fig. 7.2. Microscopic changes in the marginal area of the full-layer skin defect No. 3 with covering of wet acellular dermal matrix. Magnification: x100.* ***A****: 1 – stratified squamous nonkeratinized epithelium, 2 – parakeratosis, 3 – granulation, 4 – hemorrhage in combination with infiltrates. Hematoxylin and eosin staining.* ***B****: 1 – parakeratosis, 2 – acanthosis, 3 – blood-filled vessels, 4 – leukocyte infiltration, 5 – granulation. Hematoxylin and eosin staining.* ***C****: 1 – stratified squamous keratinized epithelium, 2 – dermis with fibrous structures. Azan III chrome stain.* ***D****: 1 – small interstitial hemorrhages, 2 – collagen fibers. Azan III chrome stain*

Therefore, assessing the quality of artificial wound dressings for cytotoxicity and biocompatibility tests with live human cells is essential. Currently, dozens, if not hundreds, of protocols for creating acellular matrices exist, reflecting an ongoing search for the optimal approach [41]. To understand the potential reasons for the observed differences in toxicity/biocompatibility, we analyzed the decellularization protocols for our two variants of dermal matrices.

As we may see, protocols differ only in the final step: either lyophilization (d-ADM) or soaking and subsequent preservation in a specialized triple solution (w-ADM) (Table 2). We may suggest that lyophilization contributes to the toxic properties of d-ADM. Probably, sublimation drying induces structural and/or chemical changes in the dermal matrix that negatively affect its properties. Investigating this issue further requires an in-depth study.

Decellularized matrices should have high biocompatibility and biodegradability to avoid inflammatory reactions in the recipient [42]. Given our future research goal to study the therapeutic efficacy of combining ADM with hU-MSCs, it was particularly relevant for us to investigate the biocompatibility of such matrices with MSCs. Despite extensive research focused on ADM's characteristics [43-45], studies examining biocompatibility with hU-MSCs remain limited [34].

The biocompatibility of w-ADM with hU-MSCs and the cytotoxicity of d-ADM observed in our studies can be explained by several potential factors related to the structural integrity, hydration status, and biophysical properties of the tested matrix variants. The w-ADM preserves the integrity of the ECM during preparation, minimizing damage to the 3D dermal structures that occur because of freeze-drying. This ensures that essential structural and biochemical components, such as collagen fibres and glycoproteins, remain intact and provide a natural microenvironment that supports cell adhesion and survival. In contrast, during lyophilization, ice crystals that form during freezing can disrupt the

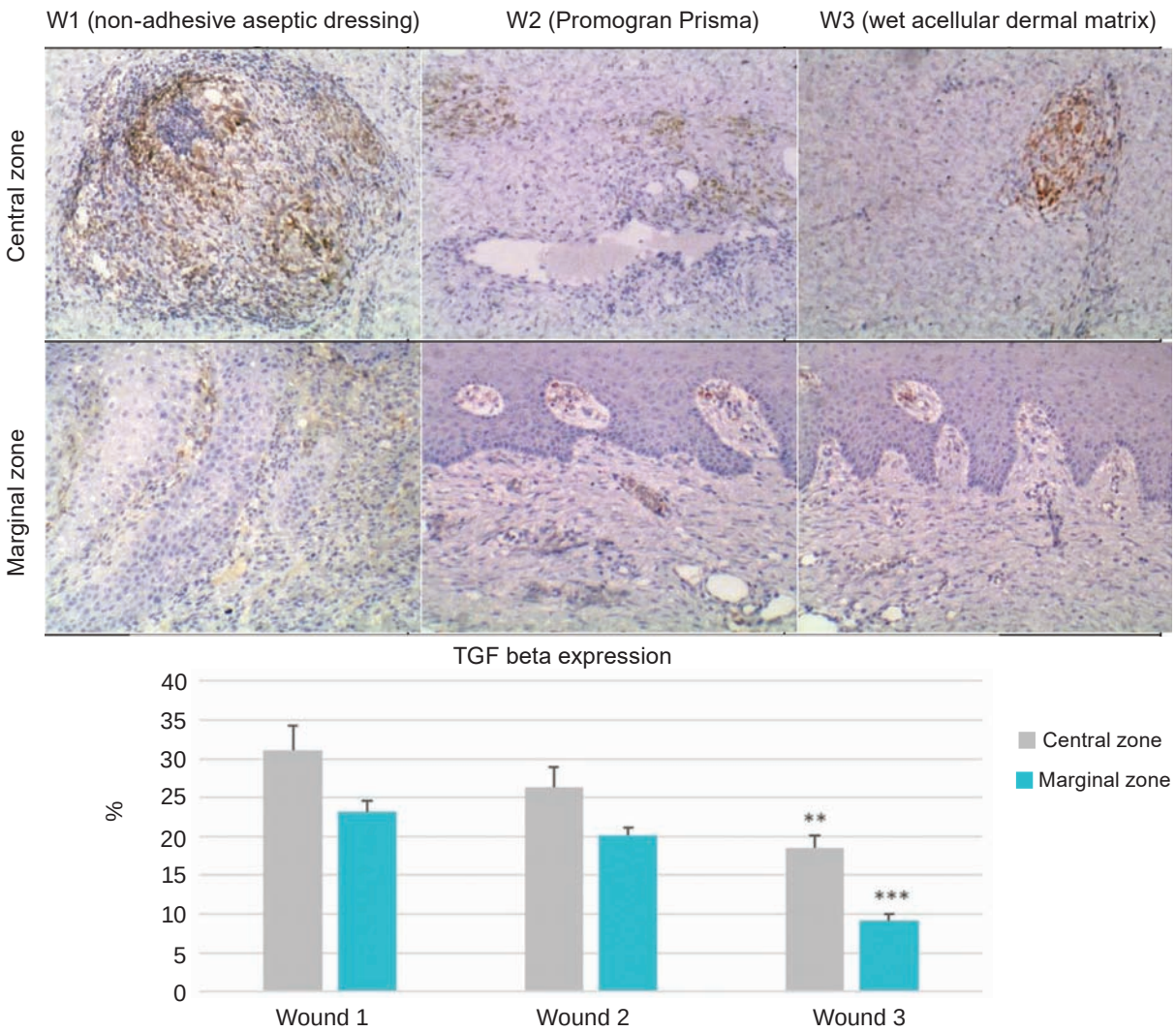


*Fig. 8. TGF-beta expression in the central and marginal areas of full-layer wounds. Detection of TGF beta+ areas in the porcine skin dermis by immunohistochemical method (100x) (A). Percentage values of TGF beta marker expression levels. *Values that were statistically significantly different from those of wound No. 1 (**P < 0.01, ***P < 0.001)*

dermal matrix at the molecular level. Additionally, drying weakens tensile strength by breaking hydrogen bonds, leading to the loss of the triple-helical structure of collagen [41].

Lyophilization also removes water from the matrix, potentially causing osmotic imbalances when cells are seeded. Conversely, w-ADM is ready to use immediately without requiring rehydration and maintains a physiological hydration level critical for hU-MSCs viability. Altered mechanical and physical properties of d-ADM may induce stress responses in MSCs, leading to apoptosis or necrosis; may exhibit altered mechanical properties that limit nutrient and oxygen supply, increasing the likelihood of cell death.

The surface properties of w-ADM are closer to native tissue, enhancing cell adhesion through integrin-dependent mechanisms. Lyophilization may alter the topography of molecules and biochemical signals, making the matrix less favorable for cell adhesion and survival. Our study demonstrated full biocompatibility and no cytotoxicity of w-ADM, which is used further for chronic wound treatment in experiments.

Dressing plays a crucial role in wound care, aimed at optimizing the wound healing environment (e.g., exudate management) and preventing infection and blistering. Our experiment on pigs demonstrated a significant benefit of w-ADM for the healing of the full-layer wound compared to non-adhesive

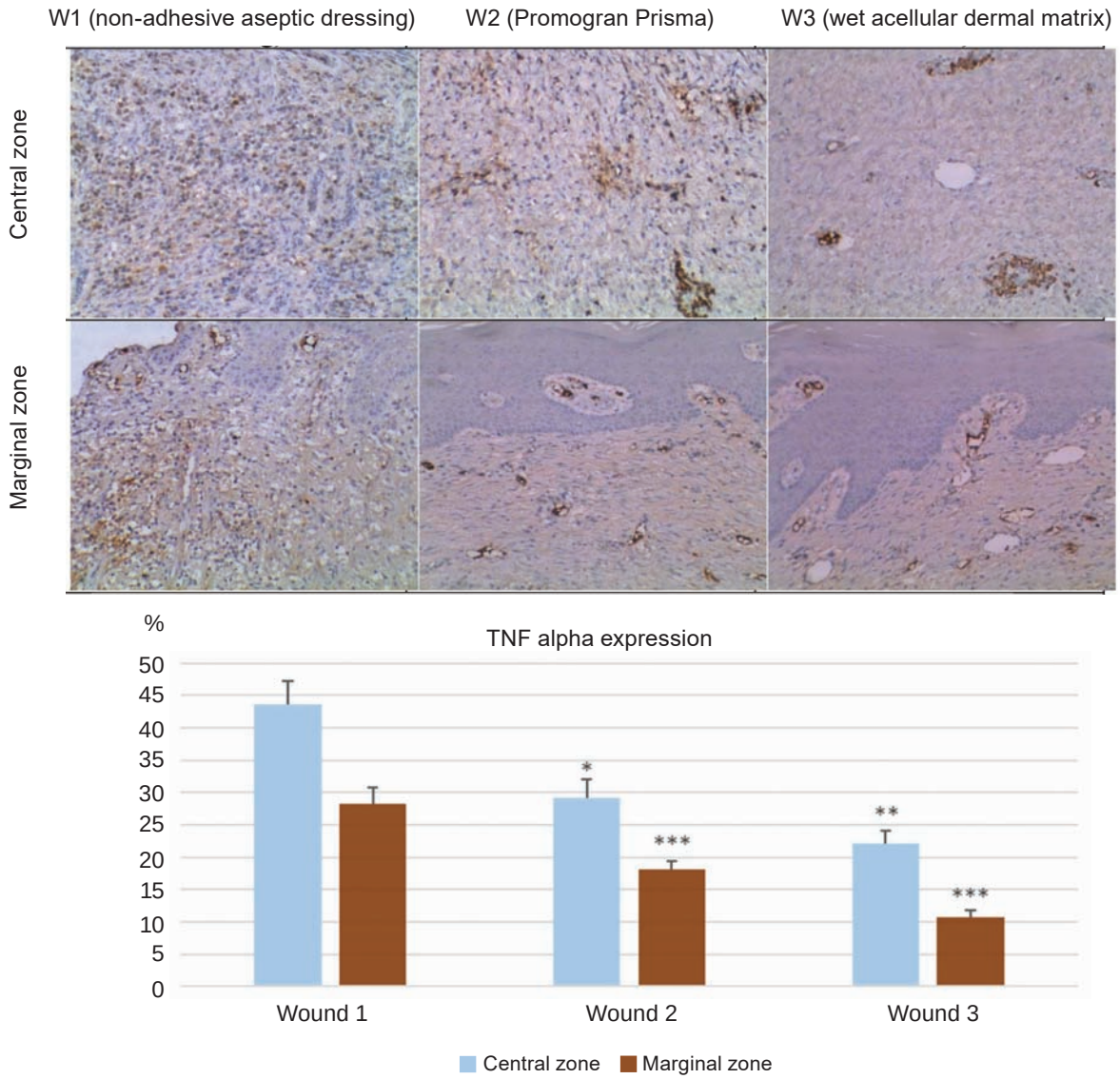


*Fig. 9. Expression of TNF alpha marker in the central and marginal areas of full-layer wounds. Detection of TNF alpha+ areas in the pig skin dermis by immunohistochemical method (100x) (**A**). Percentage values of TNF alpha marker expression levels. * Values that were statistically significantly different from those of wound No. 1 (*P < 0.05, **P < 0.01, ***P < 0.001) (**B**)*

aseptic dressing or Promogran Prizma dressing. Morphological study demonstrated that 28 days after the creation of a full-layer skin defect, w-ADM application promotes complete epithelialization of the wound surface, with restoration of the epidermal layer. The matrix helped to reduce the swelling of fibrous structures and intercellular substances, with a pronounced anti-inflammatory effect and wound healing activity.

Immunohistochemical analysis revealed a statistically significant decrease in the expression of the proinflammatory cytokine TNF-alpha and transforming growth factor TGF-beta at the wet acellular dermal matrix dressing compared to other groups, indicating its pronounced anti-inflammatory effect. The analysis of proliferative activity by the level of Ki-67 expression showed that the lowest level of mitotic activity of dermal and epidermal cells was observed with the use of acellular dermal matrix, which may indicate the stabilization of regeneration processes and the completion of the active phase of healing.

*Limitations of the study.* The study was limited to the preclinical evaluation of acellular dermal matrices without investigating their regenerative potential in combination with cell-based therapies. In

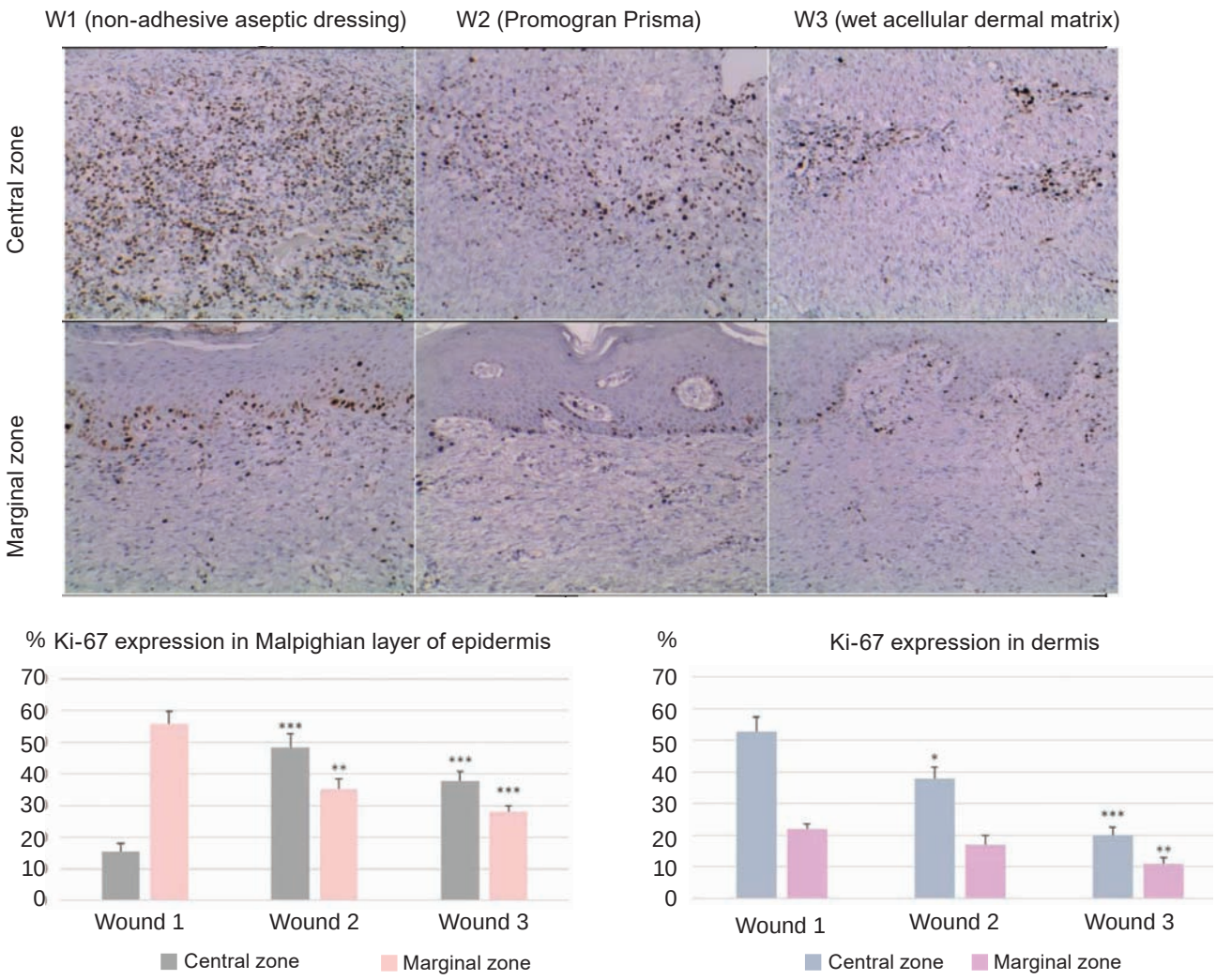


*Fig. 10. Expression of the proliferative activity marker Ki-67 in the central and marginal areas of full-layer wounds. Detection of Ki-67+ cells in pig skin by immunohistochemical method (100x) (**A**). Percentage values of Ki-67 marker expression in the epidermis and dermis. *Values that were statistically significantly different from those of wound No. 1 (*P < 0.05, **P < 0.01, ***P < 0.001)*

addition, long-term functional outcomes and the molecular mechanisms underlying tissue regeneration were not assessed. Further studies should evaluate the therapeutic performance of wet acellular dermal matrices combined with mesenchymal stem cells and validate these findings in clinical settings

*Conclusion.* The biological properties of porcine acellular dermal matrices depend on the decellularization and processing protocol. Wet ADM demonstrated full biocompatibility with human umbilical mesenchymal stem cells, whereas dry ADM exhibited cytotoxicity. In a porcine chronic wound model, wet ADM accelerated wound healing, promoted complete re-epithelialization, reduced inflammation, and improved tissue remodeling. These findings support the potential application of wet ADM as a promising biomaterial for chronic wound treatment and regenerative medicine.

*Author contributions.* All authors made a significant contribution to the work reported, whether that is in the conception, study design, execution, acquisition of data, analysis and interpretation, or in all these areas; took part in drafting, revising or critically reviewing the article; gave final approval of the version to be published; have agreed on the journal to which the article has been submitted; and agree to be accountable for all aspects of the work.

*Table 2. Comparison of decellularization protocols*

| Step | d-ADM Protocol | w-ADM Protocol |
|---|---|---|
| 1. Freeze-thaw process | Cycles in liquid nitrogen -196°C and water 37°C three times | Cycles in liquid nitrogen -196°C and water 37°C three times |
| 2. Glycerin dehydration | Immersion in 200 ml glycerin + 800 ml distilled water | Immersion in 200 ml glycerin + 800 ml distilled water |
| 3. Osmotic stress | Alternate immersion in distilled water and hypertonic solution (15-min cycles, repeated 5 times) | Alternate immersion in distilled water and hypertonic solution (15-min cycles, repeated 5 times) |
| 4. Detergent washing | 1.0% SDS washing for 4 h | 1.0% SDS washing for 4 h |
| 5. Final stage | Sublimation drying | Immersion in a triple solution (500 g of anhydrous calcium chloride + 648 ml of distilled water), Mechanical stirring. After the solution cooled, 518 ml of anhydrous ethanol was added, and the solution was heated to 38°C for 2 h in a water bath |

*Conflict of interest.* The authors have completed the Unified Conflicts of Interest form at http:// ukr-biochemjournal.org/wp-content/uploads/2018/12/coi_disclosure.pdf and declare no conflict of interest.

*Funding.* The study was funded by the Ministry of Health of Ukraine, grant # 0124U001099 “Application of regenerative medicine technologies for the treatment of chronic wounds”.

*Data availability statement*. The datasets used and/or analysed during the current study are available from the corresponding author on reasonable request.

## АЦЕЛЮЛЯРНИЙ ДЕРМАЛЬНИЙ МАТРИКС ДЛЯ ЛІКУВАННЯ ХРОНІЧНИХ РАН: СУХИЙ ЧИ ВОЛОГИЙ?

*А. І. Довгалюк*[1], *О. І. Кулянда*[2], *Н. В. Огінська*[1], *О. С. Редько*[1], *О. О. Кулянда*[3], *А. О. Ковальчук*[4], *В. В. Кульбіцька*[1], *С. Б. Крамар*[1], *З. М. Небесна*[1], *М. М. Корда*[2], *О. О. Шевчук*[5]✉

[1]Кафедра гістології та ембріології, Тернопільський національний медичний університет імені І. Я. Горбачевського, Тернопіль, Україна;
[2]Кафедра медичної біохімії, Тернопільський національний медичний університет імені І. Я. Горбачевського, Тернопіль, Україна;
[3]Кафедра патофізіології, Тернопільський національний медичний університет імені І. Я. Горбачевського, Тернопіль, Україна;
[4]Центральна науково-дослідна лабораторія, Тернопільський національний медичний університет імені І. Я. Горбачевського, Тернопіль, Україна;
[5]Кафедра фармакології та клінічної фармакології, Тернопільський національний медичний університет імені І. Я. Горбачевського, Тернопіль, Україна;
✉e-mail: shevchukoo@tdmu.edu.ua

**Вступ.** Хронічні рани становлять серйозну клінічну та економічну проблему, а їх ефективне лікування потребує нових біоматеріалів, здат-

них сприяти регенерації тканин. Ацелюлярні дермальні матрикси (ADM) є перспективними біоматеріалами регенеративної медицини, проте їхня ефективність значною мірою залежить від технології виготовлення та біологічних властивостей. **Мета.** Порівняти біосумісність і цитотоксичність двох варіантів ацелюлярного дермального матриксу, сухого (d-ADM) та вологого (w-ADM), а також оцінити терапевтичну ефективність біосумісного матриксу в експериментальній моделі хронічної повношарової рани у свиней. **Методи.** Біосумісність оцінювали *in vitro* на культурі мезенхімальних стовбурових клітин пуповини людини (hU-MSCs) за морфологією клітин, життєздатністю, проліферацією та рівнем лактатдегідрогенази (LDH). Ефективність обраного матриксу досліджували *in vivo* на моделі хронічної повношарової ексцизійної рани у свиней, порівнюючи його з неадгезивною пов'язкою та матриксом Promogran Prisma. Через 28 діб проводили гістологічне, імуногістохімічне (TNF-α, TGF-β, Ki-67) та морфометричне дослідження. **Результати.** Вологий ацелюлярний дермальний матрикс забезпечував збереження морфології, життєздатності та проліферативної активності hU-MSCs, тоді як сухий матрикс проявляв виражену цитотоксичність з підвищенням активності LDH та масовою загибеллю клітин. На моделі хронічної рани застосування w-ADM достовірно прискорювало загоєння порівняно з контрольними методами лікування, забезпечуючи повну та стабільну реепітелізацію, мінімальну запальну інфільтрацію, впорядковане ремоделювання колагену та відновлення структури тканин. Імуногістохімічно встановлено зниження експресії TNF-α, TGF-β та Ki-67, що свідчить про згасання запальної реакції та перехід процесу загоєння до стадії ремоделювання й стабілізації регенерації. **Висновки.** Вологий ацелюлярний дермальний матрикс продемонстрував високу біосумісність, відсутність цитотоксичності та значно кращі регенеративні властивості порівняно із сухим матриксом. Отримані результати підтверджують перспективність використання w-ADM як ефективного біоматриксу для лікування хронічних ран і створюють підґрунтя для подальших доклінічних та клінічних досліджень, зокрема в комбінації з мезенхімальними стовбуровими клітинами.

Ключові слова: хронічні рани, ацелюлярний дермальний матрикс, ліофілізація, мезенхімальні стовбурові клітини пупкової порожнини людини, біосумісність, цитотоксичність, морфологія.

## References

1. Jain K, Avsar P, Patton D, Moore Z, Murray B. What specific challenges do patients with chronic wounds encounter when attending medical appointments related to wound care? A systematic review. *J Tissue Viability*. 2025; 34(2): 100865.
2. McCosker L, Tulleners R, Cheng Q, Rohmer S, Pacella T, Graves N, Pacella R. Chronic wounds in Australia: A systematic review of key epidemiological and clinical parameters. *Int Wound J*. 2019; 16(1): 84-95.
3. Bowers S, Franco E. Chronic Wounds: Evaluation and Management. *Am Fam Physician*. 2020; 101(3): 159-166.
4. Atkin L, Bućko Z, Conde Montero E, Cutting K, Moffatt C, Probst A, Romanelli M, Schultz GS, Tettelbach W. Implementing TIMERS: the race against hard-to-heal wounds. *J Wound Care*. 2019; 23(Sup3a): S1-S50.
5. Fife C, LeBoutillier B, Taylor C, Marcinek BT. Real-World Use and Outcomes of Hard-To-Heal Wounds Managed With Porcine Placental Extracellular Matrix. *Cureus*. 2024; 16(12): e76262.
6. Eriksson E, Liu PY, Schultz GS, Martins-Green MM, Tanaka R, Weir D, Gould LJ, Armstrong DG, Gibbons GW, Wolcott R, Olutoye OO, Kirsner RS, Gurtner GC. Chronic wounds: Treatment consensus. *Wound Repair Regen*. 2022; 30(2): 156-171.
7. Sen CK. Human Wound and Its Burden: Updated 2020 Compendium of Estimates. *Adv Wound Care (New Rochelle)*. 2021; 10(5): 281-292.
8. Greenstein ES, Falone W, Patterson T, Cesario K, Mitchell L, Martel T, Rivera J, Vooijs M, Norton S. Treating chronic wounds in an acute care setting: the forgotten diagnosis. *Wound Manag Prev*. 2024; 70(1): 22085.
9. Martinengo L, Olsson M, Bajpai R, Soljak M, Upton Z, Schmidtchen A, Car J, Järbrink K. Prevalence of chronic wounds in the general population: systematic review and meta-analysis of observational studies. *Ann Epidemiol*. 2019; 29: 8-15.

10. Olsson M, Järbrink K, Divakar U, Bajpai R, Upton Z, Schmidtchen A, Car J. The humanistic and economic burden of chronic wounds: A systematic review. *Wound Repair Regen*. 2019; 27(1): 114-125.
11. Lim HW, Collins SAB, Resneck JS Jr, Bolognia JL, Hodge JA, Rohrer TA, Van Beek MJ, Margolis DJ, Sober AJ, Weinstock MA, Nerenz DR, Smith Begolka W, Moyano JV. The burden of skin disease in the United States. *J Am Acad Dermatol*. 2017; 76(5): 958-972.e2.
12. Sorg H, Sorg CGG. Skin Wound Healing: Of Players, Patterns, and Processes. *Eur Surg Res*. 2023; 64(2): 141-157.
13. Pang C, Ibrahim A, Bulstrode NW, Ferretti P. An overview of the therapeutic potential of regenerative medicine in cutaneous wound healing. *Int Wound J*. 2017; 14(3): 450-459.
14. Kolimi P, Narala S, Nyavanandi D, Youssef AAA, Dudhipala N. Innovative Treatment Strategies to Accelerate Wound Healing: Trajectory and Recent Advancements. *Cells*. 2022; 11(15): 2439.
15. Las Heras K, Igartua M, Santos-Vizcaino E, Hernandez RM. Chronic wounds: Current status, available strategies and emerging therapeutic solutions. *J Control Release*. 2020; 328: 532-550.
16. Marfia G, Navone SE, Di Vito C, Ughi N, Tabano S, Miozzo M, Tremolada C, Bolla G, Crotti C, Ingegnoli F, Rampini P, Riboni L, Gualtierotti R, Campanella R. Mesenchymal stem cells: potential for therapy and treatment of chronic non-healing skin wounds. *Organogenesis*. 2015; 11(4): 183-206.
17. Dai C, Shih S, Khachemoune A. Skin substitutes for acute and chronic wound healing: an updated review. *J Dermatolog Treat*. 2020; 31(6): 639-648.
18. Kulyanda IS, Fedoniuk LY, Dovgalyuk AI, Kramar SB, Kulyanda OO. Production of Acellular Dermal Matrix of Pig's Skin: Morphological Analysis. *Achiev Clin Exp Med*. 2020; (4): 107-113. (In Ukrainian).
19. Ding Z, Dan N, Chen Y. Study of a Hydrophilic Healing-Promoting Porcine Acellular Dermal Matrix. *Processes*. 2022; 10(5): 916.
20. Browne S, Petit N, Quondamatteo F. Functionalised biomaterials as synthetic extracellular matrices to promote vascularisation and healing of diabetic wounds. *Cell Tissue Res*. 2024; 395(2): 133-145.
21. Hosty L, Heatherington T, Quondamatteo F, Browne S. Extracellular matrix-inspired biomaterials for wound healing. *Mol Biol Rep*. 2024; 51(1): 830.
22. Urciuolo F, Casale C, Imparato G, Netti PA. Bioengineered Skin Substitutes: the Role of Extracellular Matrix and Vascularization in the Healing of Deep Wounds. *J Clin Med*. 2019; 8(12): 2083.
23. Solarte David VA, Güiza-Argüello VR, Arango-Rodríguez ML, Sossa CL, Becerra-Bayona SM. Decellularized Tissues for Wound Healing: Towards Closing the Gap Between Scaffold Design and Effective Extracellular Matrix Remodeling. *Front Bioeng Biotechnol*. 2022; 10: 821852.
24. Campitiello F, Mancone M, Cammarota M, D'Agostino A, Ricci G, Stellavato A, Della Corte A, Pirozzi AVA, Scialla G, Schiraldi C, Canonico S. Acellular Dermal Matrix Used in Diabetic Foot Ulcers: Clinical Outcomes Supported by Biochemical and Histological Analyses. *Int J Mol Sci*. 2021; 22(13): 7085.
25. Chen Y, Liu X, Zheng X, Huang X, Dan W, Li Z, Dan N, Wang Y. Advances on the modification and biomedical applications of acellular dermal matrices. *J Leather Sci Eng*. 2022; 4(1): 1-19.
26. Hsieh CM, Wang W, Chen YH, Wei PS, Liu YH, Sheu MT, Ho HO. A Novel Composite Hydrogel Composed of Formic Acid-Decellularized Pepsin-Soluble Extracellular Matrix Hydrogel and Sacchachitin Hydrogel as Wound Dressing to Synergistically Accelerate Diabetic Wound Healing. *Pharmaceutics*. 2020; 12(6): 538.
27. Tognetti L, Pianigiani E, Ierardi F, Lorenzini G, Casella D, Liso FG, De Pascalis A, Cinotti E, Rubegni P. The use of human acellular dermal matrices in advanced wound healing and surgical procedures: State of the art. *Dermatol Ther*. 2021; 34(4): e14987.
28. Brown M, Li J, Moraes C, Tabrizian M, Li-Jessen NYK. Decellularized extracellular matrix: New promising and challenging biomaterials for regenerative medicine. *Biomaterials*. 2022; 289: 121786.
29. Byk PL, Kryvorchuk IH, Leshchyshyn IM, Martyniuk NS, Orlov DY. Epidemiology and Antibiotic Resistance of Combat Wound Infection in Surgical Patients. *Ukr J Cardiovasc Surg*. 2024; 32(2): 129-140. (In Ukrainian).

30. Sinyuk M, Polishchuk V, Yuschak P, Burachok I. Management of war-related facial wounds in Ukraine: the Lviv military hospital experience. *BMJ Mil Health*. 2025; 171(1): 12-15.
31. Alegre MG, Lopez EM, Blasco M, Benavente VY, Roldan MDMR. Overview of pain in Ukrainian war injured. *Injury*. 2025; 56(2): 112046.
32. Seavey JG, Masters ZA, Balazs GC, Tintle SM, Sabino J, Fleming ME, Valerio IL. Use of a bioartificial dermal regeneration template for skin restoration in combat casualty injuries. *Regen Med*. 2016; 11(1): 81-90.
33. Fedoniuk LYa, Kulyanda IS, Dovgalyuk AI, Lomakina YuV, Kramar SB, Kulianda OO, Valko OO. Morphological characteristics of acellular dermal matrix manufacturing. *Wiad Lek*. 2021; 74(3 p.I): 418-422.
34. Guarnieri R, Reda R, Di Nardo D, Miccoli G, Zanza A, Testarelli L. In Vitro Direct and Indirect Cytotoxicity Comparative Analysis of One Pre-Hydrated versus One Dried Acellular Porcine Dermal Matrix. *Materials (Basel)*. 2022; 15(5): 1937.
35. Kumar P, Nagarajan A, Uchil PD. Analysis of Cell Viability by the Lactate Dehydrogenase Assay. *Cold Spring Harb Protoc*. 2018; 2018(6): pdb.prot095497.
36. Masson-Meyers DS, Andrade TAM, Caetano GF, Guimaraes FR, Leite MN, Leite SN, Frade MAC. Experimental models and methods for cutaneous wound healing assessment. *Int J Exp Pathol*. 2020; 101(1-2): 21-37.
37. Wong VW, Sorkin M, Glotzbach JP, Longaker MT, Gurtner GC. Surgical approaches to create murine models of human wound healing. *J Biomed Biotechnol*. 2011;2011: 969618.
38. Kulianda O. Experimental modelling of full-thickness skin wounds in pigs. *Bull Med Biol Res*. 2025; 7(1): 43-50.
39. Pawlak J, Trzcionka A, Mertas A, Dziedzic A, Hildebrandt T, Tanasiewicz M. The Cytotoxicity Assessment of Novel Formulation Developed to Reduce Dentin Hypersensitivity Utilizing Dehydrogenase Assay. *Coatings*. 2021; 11(2): 217.
40. Shin JW, Kwon SH, Choi JY, Na JI, Huh CH, Choi HR, Park KC. Molecular Mechanisms of Dermal Aging and Antiaging Approaches. *Int J Mol Sci*. 2019; 20(9): 2126.
41. Wang B, Qinglai T, Yang Q, Li M, Zeng S, Yang X, Xiao Z, Tong X, Lei L, Li S. Functional acellular matrix for tissue repair. *Mater Today Bio*. 2022; 18: 100530.
42. Heath DE. A Review of Decellularized Extracellular Matrix Biomaterials for Regenerative Engineering Applications. *Regen Eng Transl Med*. 2019; 5(2): 155-166.
43. Hoshiba T. Decellularized Extracellular Matrix for Cancer Research. *Materials (Basel)*. 2019; 12(8): 1311.
44. Primasari M, Saputro ID, Hariani L, Velusamy GPB. Developing Porcine Acellular Dermal Matrix by Using Sodium Dodecyl Sulfate and Biomechanical Property Testing. *Biomol Heal Sci J*. 2024; 7(1): 23-28.
45. Cheon JH, Yoon ES, Kim JW, Park SH, Lee BI. A comparative study between sterile freeze-dried and sterile pre-hydrated acellular dermal matrix in tissue expander/implant breast reconstruction. *Arch Plast Surg*. 2019; 46(3): 204-213.